Hayward, D. W., Lunn, D. J., Seddon, A., Finnegan, J. R., Gould, O. E. C., Magdysyuk, O., Manners, I., Whittell, G. R., & Richardson, R. M. (2018). Structure of the Crystalline Core of Fiber-like Polythiophene Block Copolymer Micelles. *Macromolecules*, *51*(8), 3097-3106. https://doi.org/10.1021/acs.macromol.7b02552

Structure of the crystalline core of fibre-like polythiophene block copolymer micelles

Dominic W. Hayward,[†,‡,¶] David J. Lunn,[†] Annela Seddon,[¶] John R. Finnegan,[†] Oliver E. C. Gould,[†] Oxana Magdysyuk,[§] Ian Manners,[†] George R. Whittell,[*,†] and Robert M. Richardson[*,‡]

†*School of Chemistry, University of Bristol, Bristol BS8 1TS, U.K.*

‡*H.H. Wills Physics Laboratory, University of Bristol, Bristol BS8 1TL, U.K*

¶*Bristol Centre for Functional Nanomaterials, University of Bristol, Bristol BS8 1TL, U.K*

§*Diamond Light Source, Harwell Science & Innovation Campus, Didcot, Oxfordshire OX11 0DE, U.K.*

E-mail: g.whittell@bristol.ac.uk; robert.richardson@bristol.ac.uk

Abstract

The internal structure and cross sectional geometry of fibre-like poly(3-hexylthiophene)-based block copolymer micelles has been determined using small- and wide-angle X-ray scattering (SAXS and WAXS respectively) techniques alongside electron and atomic force microscopies. WAXS of concentrated micellar solutions demonstrated that the block copolymers form crystalline-core micelles in solvents selective for the corona-forming block. Furthermore, by generating macroscopic fibres from micellar solutions, it was possible to align the micelles and discern the type and orientation of the unit cell within the core. Using the unit cell information gained from the wide-angle measurements, in conjunction with the structural insights gained from the microscopy

techniques, it was possible to form a complete picture of the cross-sectional geometry of the micelles, whereby the polymer chains lie perpendicular to the long axis of the micelle core and do not undergo chain-folding. Finally, this information was used to propose a self-assembly mechanism and to construct and validate a model for the small-angle scattering data, revealing the inherent flexibility of the micelles.

Introduction

Due to the impressive combination of stability,[1] high field-effect mobility[2] and solution processability[3] π-conjugated poly(3-alkylthiophene)s (P3AT)s have generated significant academic and industrial interest, leading to the development of P3AT-based organic electronic devices such as solar cells[4] and field effect transistors.[5] The optimisation of such devices, however, relies on either manipulating the diffusion of excitons or balancing charge carrier transport, both of which require control over the supramolecular structure.[6,7] One method for achieving this control has been through covalently linking the P3AT to a more flexible polymer chain, forming a rod-coil block copolymer. Given appropriate block lengths and processing conditions, these have been shown to phase-segregate in the bulk or thin films to form lamellar or fibre-like morphologies with crystalline polythiophene domains.[8–11] A further advantage of block copolymers over the corresponding homopolymers is the additional colloidal stability imparted by the coblock, enabling solution-based self-assembly and processing techniques.

Block copolymers with a crystallisable core-forming segment have been shown to be highly amenable to solution phase self-assembly.[12] Work done on block copolymers containing the crystalline metalloblock poly(ferrocenyldimethylsilane) (PFS)[13] for example, shows that it is not only possible to control the morphology by varying block ratios,[14,15] but also to precisely tune the dimensions via a technique known as living crystallisation-driven self-assembly (living CDSA).[16] Using synchrotron small- and wide-angle X-ray scattering (SAXS and WAXS respectively) it was possible to determine both the crystal structure and cross-sectional geom-

etry of the micelle core.[17] The high degree of morphological and length control coupled with knowledge of the internal structure subsequently enabled the fabrication a wide variety of complex nano-architectures including patchy micelles,[18] branched micelles,[19] supermicelles[20] and even cross supermicelles.[21] This technique is not just limited to metalloblocks; recently an expanding number of di- and triblock copolymers that contain crystalline components have been shown to self-assemble in solution to afford cylindrical or elongated structures with dimensional control, including: polyethylene,[22–25] poly(ϵ-caprolactone),[26,27] polythiophenes,[28–34] polyselenophene,[35] poly(phenylene vinylene),[36] and smectic liquid crystalline polymers.[37] In principle, these materials should also serve as effective building blocks for the construction of 1-D nanostructures by living CDSA. In the case of P3ATs however, seeded growth was limited to lengths < 320 nm,[31] and growth via self-seeding to < 700 nm.[32] To understand these observations and be able to further develop this technique, it is first necessary to elucidate the internal structure and micelle morphology.

Previous work on the solution phase self-assembly of P3AT-based block copolymers in solvents selective for the amorphous corona-forming block have tended to result in fibre-like micelles, as characterised via transmission electron microscopy (TEM) or atomic force microscopic (AFM) imaging techniques.[9,38,39] A similar morphology is also found in P3AT block copolymers self-assembled in good solvents,[8,40,41] solvent mixtures[42,43] via solvent or temperature annealing[10,11,44] and from a polymer melt.[9] X-ray or electron diffraction experiments have indicated a crystal structure similar to that found in bulk P3AT homopolymer,[8,9,11] however, the orientation of the unit cell with respect to the micelle could only be inferred rather than measured directly. Small-angle scattering of P3AT-based micelles in solution has not been attempted to date. In this paper, TEM, AFM, solution SAXS and solution and fibre WAXS were conducted in order to form a complete picture of the internal and cross-sectional structure and self-assembly mechanisms of P3AT-based block copolymer micelles, which provides insight into the self-assembly mechanism. It is hoped that this investigation will inform and stimulate future work on the optimisation of P3AT-based block copolymer

structures formed in solution.

Results

Synthesis and Self-Assembly

The block copolymers used in this investigation were synthesised using previously reported methods[31,32,45–47] and a full account of the synthesis and characterisation is given in the Supporting Information. Briefly, the P3HT block was prepared via Grignard metathasis of 2,5-dibromo-3-alkylthiophene and the resultant polymer was end-functionalised with an alkynyl group. This was then coupled with the azide-terminated coblock prepared via a living anionic polymerisation in a separate step. The diblock copolymers were then dissolved in tetrahydrofuran (THF) and passed through a size-exclusion chromatography (SEC) column in order to remove the unreacted P3HT homopolymer. The relative amounts of homopolymer impurity remaining in the block copolymer (BCP) material after purification were determined, via an analysis of the gel-permeation chromatography (GPC) chromatograms, to be 4% and less than 1% for the P3HT-*b*-PS and P3HT-*b*-PI materials respectively (details and further discussion are provided on page S15 of the Supporting Information). Table 1 shows an overview of the measured block lengths and polydispersities. The micelle self-assembly was carried out according to the self-seeding protocols formulated by Qian *et al.*[32] It should be noted that the focus of this work is on the structure of the core and the cross-sectional geometry, the micelle lengths and length polydispersities were therefore not studied in detail, but fall in the range 100-1000 nm.

Wide-Angle X-ray Scattering

In order to measure the crystal structure of the polythiophene core and, in particular, the orientation of the unit cell, it was originally intended align a lyotropic liquid crystalline micelle dispersion in an electric-, magnetic- or flow-field. As this was not possible, due to

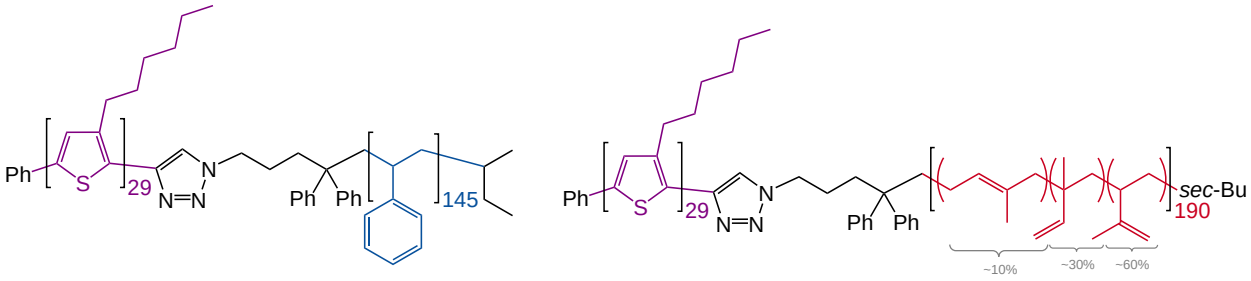

Poly(3-hexylthiophene) - *block* - Polystyrene
(P3HT - *b* - PS)

Poly(3-hexylthiophene) - *block* - Polyisoprene
(P3HT - *b* - PI)

Figure 1: Structures of the copolymers used in this work.

the absence of any observed liquid crystalline phases (*vide infra*), an alternative method was required to produce the required alignment. Inspired by the strong alignment achieved by the extrusion of molten P3HT homopolymer to form macroscopic fibres,[48,49] highly concentrated micelle dispersions (150 mg/mL) were produced by slowly allowing solvent to evaporate from stock solutions of known concentration. For $P3HT_{29}$-*b*-PS_{145} at 150 mg/ml, the solution was sufficiently viscous and amenable to fibre formation such that extended macroscopic micellar fibres could be drawn from solution using the tip of a hypodermic needle. The $P3HT_{29}$-*b*-PI_{190} material was not conducive to fibre formation by this means, which is probably due to the low glass transition temperature of the PI. From scanning electron microscopy (SEM) measurements, the fibres were determined to be 8-9 μm in diameter (Figure S10). The internal structure of the micelles was then determined using wide-angle X-ray scattering (WAXS) measurements. Results from the P3HT-*b*-PS fibre are shown in Figure 2 and it can immediately be seen that the internal structure is well aligned.

Table 1: Summary of polymer characterisation data.

	M_n P3HT block	PDI	M_n coblock[a]	PDI[a]	block ratio[b]	diblock PDI[a]
$P3HT_{29}$-*b*-PS_{145}[d]	4 900[c]	1.05[c]	15 100	1.09	1:5	1.09
$P3HT_{29}$-*b*-PI_{210}	4 900[c]	1.05[c]	14 300	1.08	1:7.2	1.16

[a] Determined by triple detection GPC analysis. [b] Determined by ratio of M_n(P3HT block) and M_n(coblock). [c] Determined by MALDI-TOF MS. [d] Numbers in subscript denote the number average degree of polymerization.

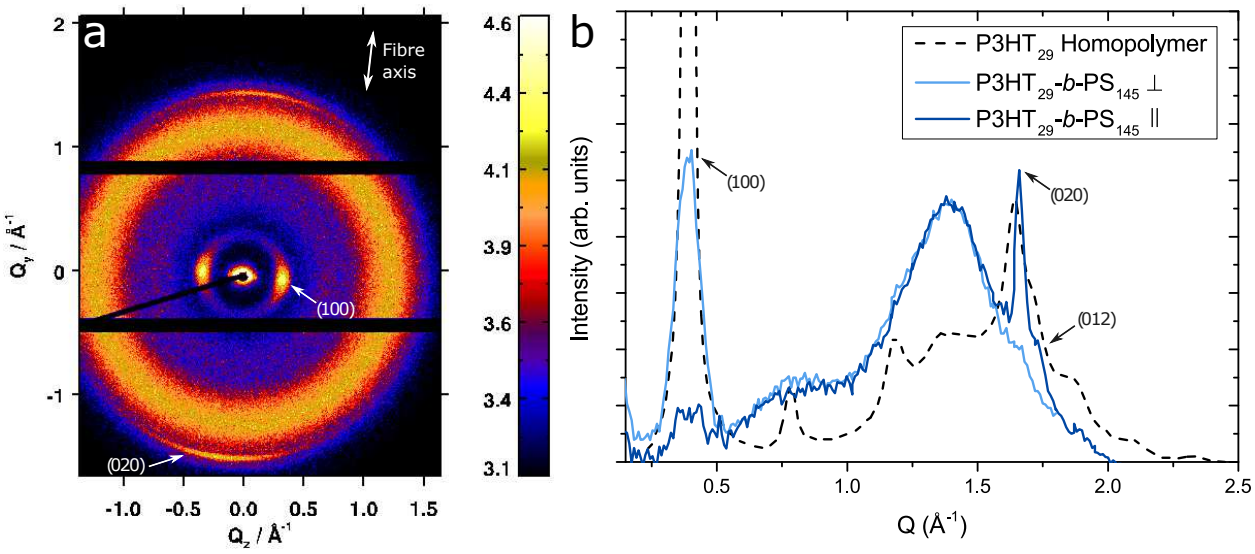

Figure 2: (a) Wide-angle scattering pattern from fibre composed of P3HT$_{29}$–*b*–PS$_{145}$ micelles. (b) Corresponding azimuthally integrated data taken from 10° segments oriented perpendicular to the fibre axis (0°) and parallel to the fibre axis (90°). Also shown for comparison is the wide-angle scattering from the precursor material P3HT$_{29}$ integrated over 360°.

By simultaneously fitting all of the observable peaks in the azimuthally regrouped data, both crystalline and amorphous, to a series of Pearson Type VII distributions using a non-linear Levenberg-Marquardt algorithm via the *Origin* software package, it was possible to extract peak positions and widths. Analysis of the crystalline peak positions and symmetry of the scattering pattern, revealed a monoclinic unit cell, shown in Figure 3, as has previously been found in bulk and thin film P3AT materials[50–53] and predicted by *ab-initio* calculations.[54] The lattice constants were found by refining the unit cell (details in the Supporting Information) and are given in Table 2. The indices for the most prominent peaks are shown in Figure 2(a). The orientation of the (100) peaks perpendicular to the fibre draw axis indicates that the a vector of the unit cell is perpendicular the draw direction of the fibre. Similarly, the orientation of the (020) peaks parallel to the fibre axis indicates that the b vector is parallel to the draw direction. Importantly from an applications perspective, this means that the π-stacking direction is along the fibre axis and the polythiophene chains (along the c direction) are also oriented perpendicular to the draw direction. To determine

Table 2: Summary of fitting to wide-angle scattering data. The uncertainties on the coherence length values were calculated by propagating the uncertainties associated with the peak widths, determined by the fits.

Material	Unit cell dimensions (nm) a	b	c	γ	Coherence Lengths (nm) d_{100}	d_{020}
$P3HT_{29}$-*b*-PS_{145}						
Fibre	1.62	0.76	0.74	93.1	4.3 ± 0.1	10.6 ± 0.7
Dry Film	1.62	0.77	0.74	94.5	5.2 ± 0.1	15.5 ± 1.1
In Solution	1.71	0.76	0.75	95.7	3.0 ± 0.1	12.1 ± 2.2
$P3HT_{29}$-*b*-PI_{190}						
Dry Film	1.72	0.77	0.74	95.6	2.7 ± 0.1	12.6 ± 1.4
In Solution	1.77	0.78	0.76	97.4	2.9 ± 0.1	7.7 ± 2.2
$P3HT_{29}$ Homopolymer						
Dry	1.61	0.77	0.71	95.1	14.7 ± 0.1	4.9 ± 0.1

the degree of orientation of the micelles within the fibres, the data around the (100) peak were radially regrouped and analysed[55] using Hermann's orientation parameter:

$$S = \frac{1}{2}\left\langle 3\cos^2\theta - 1 \right\rangle \tag{1}$$

where θ is the angle of misorientation with respect to the draw axis. The value of 0.53 for the P3HT-*b*-PS fibre indicates good alignment and is comparable to pure P3HT fibres extruded from the melt phase at high temperatures (0.45-0.78).[48,49]

To investigate how the crystal structure in the micelles differs from the precursor $P3HT_{29}$ material and whether it is affected by the drying or fibre-drawing process, WAXS measurements were also carried out on dry micelle and P3HT homopolymer films, drop cast onto a Kapton substrate from high concentration samples (100 mg/mL) of micelles in solution. The azimuthally averaged data and fits are shown in Figure 2 (homopolymer) and Figure S11. The unit cell dimensions are generally in good agreement with literature values for equivalent bulk[51–53,56] and thin film[50] P3HT. Although the unit cell dimensions of the micellar material and the homopolymer are very similar, it can be seen in Figure 2(b) that whilst the homopolymer exhibits a strong (100) reflection, as well as clearly identifiable 2nd

and 3rd order peaks, the (100) reflection in the micellar material is much broader and the higher order peaks are almost entirely absent in all of the samples measured. This indicates that the crystalline core of the micelles is short in the (100) direction. There is also a slight increase in the unit cell dimensions, particularly along the (100) axis, to larger values in solvated systems compared to dry micelle fibres and films, suggesting a small degree of solvent penetration into the alkyl chains of the P3AT. In order to quantify the approximate extent of the crystalline domains in the micelle core, the Scherrer formula for peak broadening has been applied:

$$L = \frac{5.57}{\Delta Q} \tag{2}$$

where ΔQ is the FWHM (full width at half-maximum) of the peak and L is the coherence length of the crystalline domains in the direction perpendicular to the Bragg planes. The extent of the crystalline domains may be dictated either by finite size effects, in which case the coherence length equates to the physical dimensions of the sample, or alternatively imperfections in the crystalline correlation. From the AFM and SAXS results (*vide infra*), the peak broadening along the (100) axis has been ascribed to finite size effects and it can be seen from Table 2 that this implies a micelle thickness of only two or three non-interdigitated P3AT chains. The size of the crystalline domains in the homopolymer material along the (100) axis is equivalent to approximately nine layers of chains which would explain the absence of strong higher order peaks in the micellar material. As the TEM images in Figure 4 (a,d) show ribbon-like structures extending over 100 nm, the broadening of the (020) peaks must be due to imperfections in the π-π stacking. In this case, the coherence length in the micellar material is larger, equivalent to 20-40 π-stacked chains, much larger than the stacks of $\sim$13 chains in the homopolymer film. These results show that the addition of the corona-forming block and the subsequent self-assembly in the selective solvent inhibit layer formation in the (100) direction and aid the formation of ribbons with long, coherent π-stacked domains. A schematic of the postulated self-assembled structure is given in Figure 3.

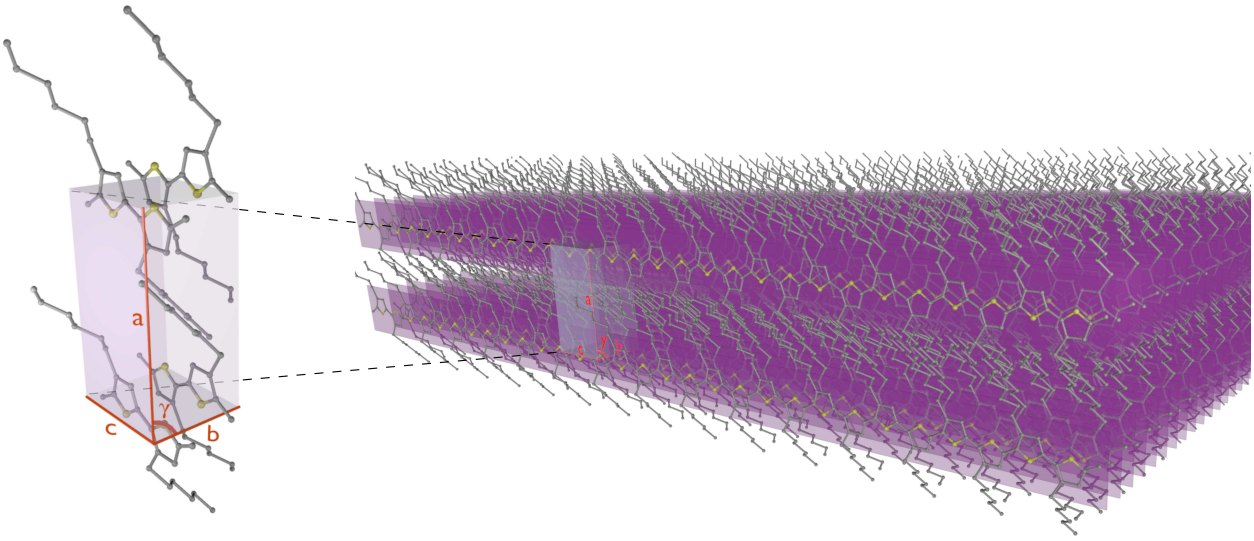

Figure 3: The derived monoclinic unit cell for the P3HT micelle cores and schematic of two layers of π-stacked $P3HT_{29}$. The fibre draw axis is parallel to the b vector.

Transmission Electron Microscopy

Although the (012) peak is sufficiently prominent to allow for the extraction of the lattice parameter c (along the axis of the polythiophene chains), there are no strong Bragg reflections from the (00l) lattice planes. Consequently, it was not possible to determine a coherence length along the c-direction from the WAXS data. In order to determine the micelle dimensions along the axis of the polythiophene chains and indeed to confirm that the structures analysed in the WAXS measurements were in micellar form, the self-assembled structures were imaged using transmission electron microscopy (TEM). The transmission electron micrographs, shown in Figure 4, confirm that in solvents selective for the corona-forming block, the polythiophene-containing block copolymers form polydisperse fibre or ribbon-like structures. In the higher magnification images, the visibility of the grains that comprise the amorphous carbon film beneath the polythiophene micelles, suggests that the structures are thin in the out-of-plane direction, in line with the short coherence length along the (h00) direction determined from the WAXS data. Taking the FWHM of the intensity values from individual pixels (Figure S12), the width of the fibres was estimated to be approximately

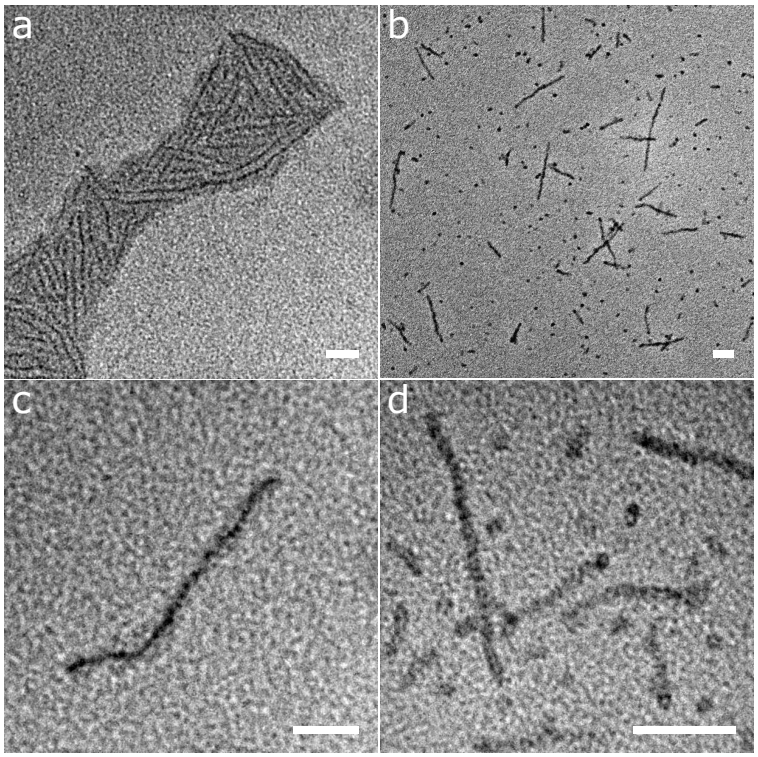

Figure 4: TEM images of self-assembled polythiophene-based block copolymers. (a) and (c) P3HT$_{29}$-*b*-PS$_{145}$ self-assembled in butyl acetate, (b) and (d) P3HT$_{29}$-*b*-PI$_{210}$ self-assembled in hexane. Scale bars represent 100 nm.

10-13 nm, commensurate with the contour length for a fully extended polythiophene chain (L_{29}: 10.7 nm, L_{31}: 11.9 nm). Theses values were calculated by multiplying the number average degree of polymerisation by c/2, as determined from WAXS measurements.

Despite the self-seeding protocols employed to control the micelle lengths, it can be seen in Figure 4 that the micelles with polyisoprene coronae are subject to a high degree of length polydispersity. The relatively poor self-assembly properties of P3HT$_{29}$-*b*-PI$_{210}$ are in marked contrast to those of PFS-*b*-PI, a material which has consistently been used to produce monodisperse near-cylindrical micelles over a wide range of block ratios.[17,57,58] The reasons for this difference may be explained with reference to the respective solubility parameters of the polymers and the solvents. Briefly, if a polymer and a solvent have similar solubility parameters, they are likely to be miscible and *vice-versa*. In this case, the solubility of P3HT in hexane is expected to be very poor (δ_{P3HT}: $\sim$19 MPa$^{1/2}$; δ_{hexane}: 14.9 MPa$^{1/2}$)[59,60]

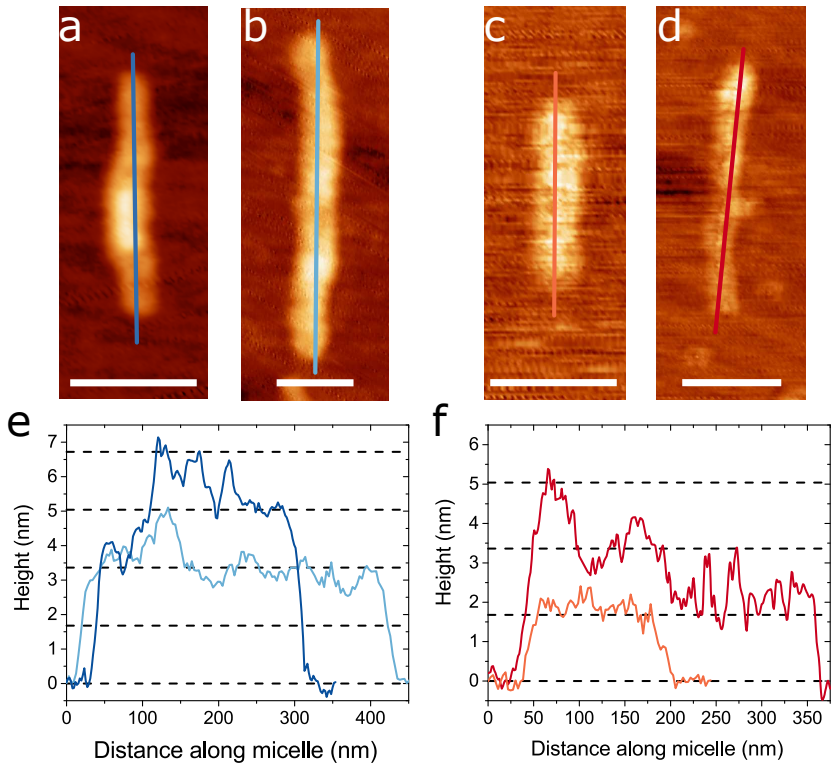

Figure 5: AFM images (a-d) and height profiles (e,f) of self-assembled polythiophene-based block copolymers. (a, b and e) $P3HT_{29}$–*b*–PS_{145}, (c, d and f) $P3HT_{29}$–*b*–PI_{210}. Scale bars represent 100 nm.

relative to that of PFS. Butyl acetate (17.4 $MPa^{1/2}$)[60] has a closer solubility parameter to that of P3HT, and the structures self-assembled in this solvent exhibits a greater proportion of elongated micelles to short micellar fragments than is observed in hexane (Figure 4). A mechanism for this is proposed in the discussion section. Attempts to improve the solubility of the P3HT block further by addition of another miscible solvent resulted in appreciable amounts of non-crystallised block copolymer unimer in solution.

Atomic Force Microscopy

In order to quantify the dimensions of the polythiophene cores along the (100) axis, the micelles were also imaged using atomic force microscopy (AFM). Representative AFM images for each of the materials, shown in Figure 5, confirm that the micelles are thin in the

out-of-plane direction, with thicknesses varying between 1.6 and 7.0 nm. Using the unit cell dimensions from the WAXS data *vide supra*, it is possible to quantify the number of polythiophene lamellae that comprise the micelle thickness. The maximum number of layers in each micelle is relatively consistent between the different core- and corona-forming materials, varying between 1 and 4 for all micelles measured, being similar to the solid-state nanofibres formed from other P3AT and P3AT block copolymer systems.[11,61] This is thought to be a direct result of the self-assembly process; in contrast to PFS-based block copolymers which undergo chain folding on addition to the micelle ends, forming extended cylinders,[16,62] P3HT chains below a molecular weight of approx. 10 kDa do not chain fold, instead forming lamellar crystals via the stacking of fully-extended chains.[61] Density functional theory (DFT) calculations on the self-assembly of P3HT homopolymers have found that, at finite temperatures, the energy associated with interactions between hexyl chains is $\sim$5 times lower than that associated with $\pi - \pi$ interactions.[63] Thus, when the $\pi - \pi$ interaction is sufficiently strong to overcome any tendency for the hexyl chains to interdigitate, the extended polythiophene chains self-assemble to form stacks in the direction orthogonal to the aromatic rings. These stacks were then shown by molecular dynamics to assemble further into layers with the hexyl chains comprising the two largest surfaces. The energy gain associated with each subsequent lamination of these layers only increases rather slowly with the addition of each layer.[63] This is expected to favour a low degree of aggregation with significant polydispersity for low concentrations.[64] It is worth considering this two step self-assembly process in light of previous work identifying a tendency of P3HT-based block copolymers to undergo homogeneous nucleation in solution.[30] This would initially give rise to a polydisperse population of unilamellar π-stacks which would gradually assemble into ribbons with incomplete layers. Such behaviour would explain the observations that not only does the thickness of the micelles vary between integer numbers of lamellae along their length, but also that the steps in thickness are 10s to 100s nm long.

Small-Angle Scattering

Finally, with a view to characterising the micelle morphology at an ensemble level, SAXS and SANS measurements were made on low concentration micelle solutions (5 mg/mL). In order to extract the micelle dimensions, it is necessary to construct an appropriate model that captures the features of the experimental data. Based on the WAXS, TEM and AFM observations, as well as previous small-angle scattering studies on similar systems by Newbloom *et al.*,[65] four models were constructed to fit the data: rigid rods with rectangular cross-sections, rigid rods with rectangular cross-sections and a corona extending on either side, rigid rods with rectangular cross-sections, an extended corona and polydispersity in the thickness direction and finally, the flexible rods with rectangular cross-sections, an extended corona and polydispersity in the thickness direction. A full description of the models is given in pages S16 - S20 of the Supporting Information and a graphical representation is shown in Figure 6. Fitting was carried out using a non-linear least-squares method allowing the core thickness, core width and scaling factor to vary (along with the polydispersity in thickness, corona length and persistence length where included). All other parameters were held constant. The azimuthally averaged data and model fits for the P3HT-*b*-PS micelles are shown in Figure 7a. In order to establish whether the fitted parameters could be reproduced in other, similar models and were not artefacts resulting from the approximations and construction of this particular model, the same data were fitted to a model for flexible

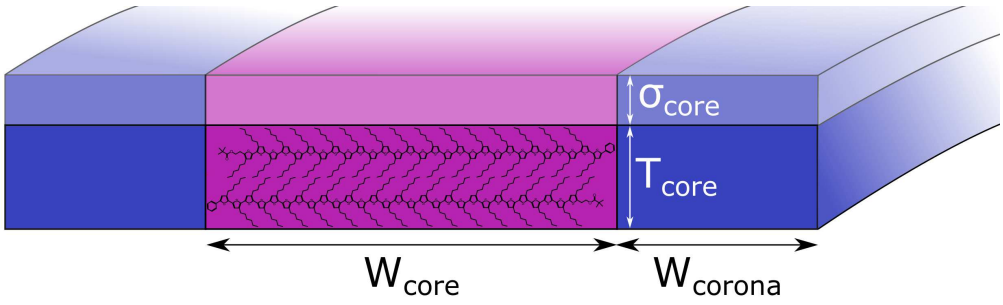

Figure 6: Scheme outlining the parameters in the model used to fit the SAXS data. Not shown in the scheme is the persistence length, a measure of the flexibility along the length of the micelle.

rods with elliptical cross-sections in the *SasView* fitting programme. The fits are shown in Figure 7b. It can immediately be seen in Figure 7a that it is not possible to accurately capture the features of the data without accounting for flexibility in the model. Figure 7b shows that the fits to an elliptical cross-section and a rectangular cross-section give almost identical results. The fitted parameters, given in Table 3, indicate that the models are in agreement on both the dimensions and degree of flexibility. With an overall aspect ratio of over 10:1, it can be expected that scattering from rods with very elliptical cross-sections and rods with polydisperse rectangular cross-sections will appear very similar and based on the fits in Figure 7b alone, it is not possible to distinguish the models. However, given that there is a near-cuboidal monoclinic unit cell in the core and no evidence of chain folding, coupled with good agreement of the TEM and AFM results with the fitted parameters for the thickness and width, a rectangular cross-section with an extended corona is considered the most likely morphology in solution. It should be noted that the fitted values indicate that the corona is shorter than the core, despite having a longer contour length. This may be due to a number of factors: firstly, the corona blocks are present in the form of two fringes whilst there is only one core. Secondly, these fringes are not crystalline and may spread out above and below core. Finally, for simplicity, the corona chain density was fitted as a block of uniform density. In reality the corona will become very diffuse towards the ends of the fringes, so the 6.7 nm will be an underestimate of the furthest extent of the corona.

The micelle dimensions in Table 3 suggest that, in line with the WAXS, TEM and AFM results, the micelles are indeed very thin. As the electron density of the hexyl chains is very close to that of the solvents, they will, to a certain degree be contrast matched in the scattering data. Under this assumption, the reported thickness of $\sim$1.7 nm for the P3HT materials would correspond to micelles with two layers of polythiophene. Fitting the persistence length gives a value of 2.7 nm and given that the core is crystalline in solution and P3AT chains are relatively rigid along their backbone, it is likely that this flexibility manifests along the micelle length. In view of the of the low values determined for the core

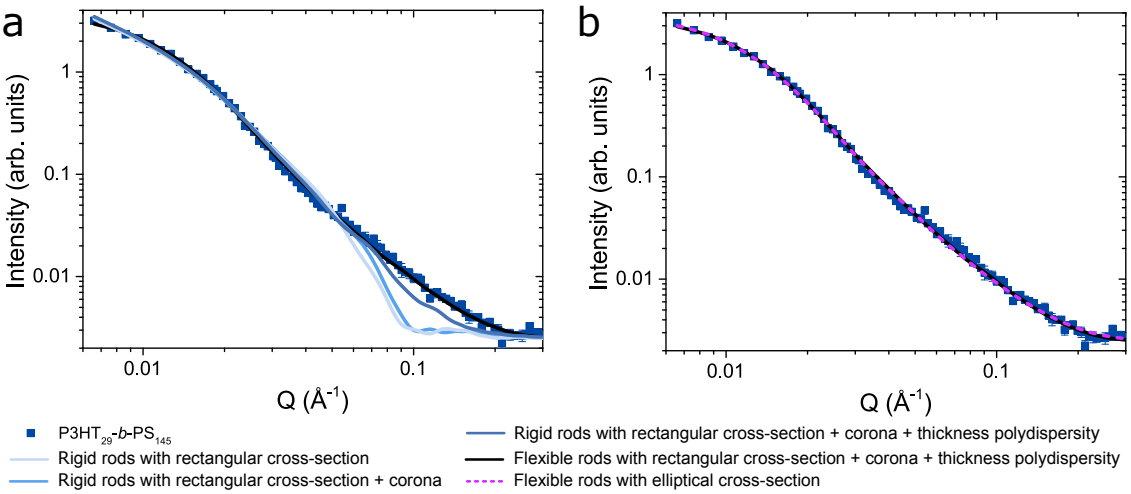

Figure 7: Plots of azimuthally averaged intensity vs Q from the small-angle scattering for 5 mg/mL dispersions of P3HT-*b*-PS micelles. The lines are fits to the data using the models described in the text. (a) shows a comparison of the models featuring rectangular cross-sections and (b) shows the comparison between the flexible rectangular and flexible elliptical models.

thickness and the well-solvated coronae, it is perhaps not surprising that the micelles are flexible in solution. This is however, in marked contrast to PFS-based cylindrical micelles where persistence lengths are of the order of 1 μm,[57] and rigidity is conferred by chain-folding within the core and the formation of a near circular cross-section.

Small-angle scattering was also conducted on the P3HT-*b*-PI micelles however, it was not possible to fit the data to the model outlined above without either appreciable discrepancies at the higher scattering vectors or implausibly small core widths. This is likely due to the presence of the shorter micelle fragments visible in Figure 4, which are not accounted for in the model. For completeness, the data and fitted parameters are given in Figure S13 and Table S1 respectively.

To determine the presence and nature of any lyotropic liquid-crystalline phases such as those observed in PFS-based systems,[66,67] SAXS and polarising optical microscopy (POM) measurements were also made on samples with higher concentrations (25, 50 and 100 mg/mL). None of the samples measured showed any optical birefringence or long-range order, nor did they exhibit any alignment in electric fields up to 8 Vμm^{-1} or in flow cells with shear rates

Table 3: Comparison of parameters fitted to P3HT-*b*-PS small-angle scattering data using different models.

Model	Parameter	Value (nm)
Flexible rods with elliptical cross-sections		
	Minor axis	1.8 ± 0.2
	Major axis	23.6 ± 2.8
	Persistence length	2.7 ± 0.2
Flexible rods with rectangular cross-sections		
	Thickness	1.7 ± 0.1
	Thickness Polydispersity	0.2 ± 0.1
	Width	11.0 ± 1.6
	Corona Length	6.7 ± 1.4
	Persistence length	2.8 ± 0.3

up to approximately 20 s^{-1}. The absence of any liquid crystalline phases was ascribed to the high degree of flexibility in the micelles. This is very different to the behaviour of the more rigid PFS system.[67]

Discussion

The fibre-like, ribbon or lamellar structure of the P3HT-based block copolymer systems studied in this work agrees well with the findings of previous studies on polythiophene block copolymer self-assembly in thin film,[8,10,40,68–71] bulk[9,11,72] and solution states.[29–32] Not only do these materials share a common general morphology, they also share a number of more subtle common features: they are usually not straight, they have rough, irregular edges and although it is neither quantified nor commented upon, in most cases, AFM images appear to shown that the thickness of the structures is not constant. In light of the structure proposed in this work, these features can be easily explained: the fibres are not straight as they are inherently very flexible, they have rough edges as the polythiophene chains are fully extended and due to polydispersity are not all of equal length, and the thickness is not constant as the $\pi - \pi$ stacking is energetically more favourable than the 'laminating' interaction between the alkyl chains.

It is also instructive to revisit the results of previous solution-based growth experiments. Using seeded growth, whereby block copolymer in a small amount of common solvent is added to a population of seed micelles in a solvent selective for the corona-forming block, it is only possible to obtain short (< 300 nm) fibres. As the selective solvent is poor for the polythiophene block, this results in a large initial interfacial free energy in the polymer-solvent system, and therefore a higher driving force for phase separation and a concomitant higher energy barrier for reorganisation. The effects of this are thought to be two-fold; firstly, this increases the likelihood of homogeneous nucleation, and secondly, as the energy barrier to rearrangement is higher, any mismatch or defects due to different orientations or chain lengths are frozen into the structure. In addition, in order to minimise unfavourable polythiophene-solvent interactions, it is energetically favourable for the well-solvated block to cover the exposed micelle ends, which will also have the effect of slowing the micelle growth. Together, these effects result in the observed short fibres and ultimately explain the limited efficacy of the seeded growth method. It is worth noting that these arguments are, in principle, applicable to any block copolymers with a crystallisable core-forming segment including those that are amenable to the seeded growth technique (e.g. PFS-based micelles). A key difference between these systems is the crystal structure; PFS chains undergo chain folding on addition to the micelle ends and form a quasi-hexagonal crystalline structure in the core,[62] the energy barrier to the reorganisation of small chain segments within the core is therefore much lower than for the analogous P3HT-based block copolymer which does not undergo chain folding at the molecular weights studied. Furthermore, as a consequence of the respective symmetries of the two unit cells, PFS self-assembles via, in essence, a one step process, whereas that of P3HT requires two steps, and the energy associated with lamination (thickness) is not independent of size. It would appear that this latter physical circumstance is not conducive to the formation of uniform structures.

In contrast to the seeded-growth method, the self-seeding approach, whereby the block copolymer is heated to dissolve the less well crystallised portion of the fibres and then slowly

cooled in a marginal solvent, results in much longer fibres. In this case, the thermal energy supplied to the system allows the polythiophene chains to reorganise and such that they do not become kinetically trapped in a less well-ordered metastable state.[32,73] Similar arguments also apply for self-assembly via dialysis into a selective solvent and slow evaporation of a good solvent from a mixture of good and selective solvents.[31]

Summary

A detailed study of the crystal structure and morphology of self-assembled P3HT-containing block copolymer micelles has been conducted using small- and wide-angle X-ray scattering, TEM and AFM characterisation techniques. By taking advantage of the strong alignment of the micelles in fibres drawn from a concentrated solution of $P3HT_{29}$-*b*-PS_{145}, it was possible to determine that the P3HT chains pack into a monoclinic unit cell with the π-stacking direction along the length of the micelles. Furthermore, it was found that, compared to the $P3HT_{29}$ precursor, the coherence lengths of the crystalline domains in the micelles along the π-stacking direction is enhanced by a factor of 2-3 compared to that in $P3HT_{29}$ films, and this persists in solution. From TEM measurements it was established that the width of the micelles is approximately equal to the contour length of the polythiophene chains which indicates that the P3AT materials do not undergo chain folding. Finally, the AFM and SAXS results revealed that the micelles are very thin, not of uniform thickness and very flexible in solution.

Viewed in concert, these results present a rather complex picture of polythiophene-containing block copolymer micelles. As opposed to the near-cylindrical structures most commonly formed by the analogous PFS-containing block copolymers, P3HT micelles form long, flexible ribbon-like structures with rectangular cross-sections of varying thickness and are much less robust than their PFS counterparts.

This picture has provided an insight into the self-assembly mechanisms of P3HT-containing

micelles and is placing DFT calculations on a firmer experimental basis. The results gained in this study also highlight the importance of the solubility of P3HT in the selective solvent and will inform future studies on tuning micelle properties. Using the methods outlined in this paper it will be possible to directly relate the self-assembly parameters of any block copolymer micelles formed via CDSA (e.g. solvent composition, annealing temperature, cooling rates etc.) to the crystal structure and morphology of the resulting micelles. By forming well-aligned fibres it should also be possible to perform macroscopic measurements on the mechanical strength and electronic properties of the micelles, which will be of particular importance for applications.

Acknowledgement

D.W.H. and O.E.C.G. were supported by EPSRC doctoral training centre grant [EP/G036780/1]. D.J.L. was supported by EPSRC doctoral training centre grant [EP/G036764/1]. The authors gratefully acknowledge the Diamond Light Source synchrotron facility for a beamtime award (experiment EE10283-1). TEM studies were carried out in the Chemistry Imaging Facility at UoB with equipment funded by UoB and EPSRC (EP/K035746/1 and EP/M028216/1). The Ganesha X-ray scattering apparatus used for this research was purchased under EPSRC Grant "Atoms to Applications" grant [EP/K035746/1].

Supporting Information Available

Experimental procedures, additional characterisation data and a detailed description of the model used to fit the small-angle scattering data can be found in the supporting information.

This material is available free of charge via the Internet at `http://pubs.acs.org/`.

References

(1) Jørgensen, M.; Norrman, K.; Gevorgyan, S. A.; Tromholt, T.; Andreasen, B.; Krebs, F. C. Stability of Polymer Solar Cells. *Advanced Materials* **2012**, *24*, 580–612.

(2) Bao, Z.; Dodabalapur, A.; Lovinger, A. J. Soluble and processable regioregular poly(3-hexylthiophene) for thin film field-effect transistor applications with high mobility. *Applied Physics Letters* **1996**, *69*, 4108.

(3) Sun, S.; Salim, T.; Wong, L. H.; Foo, Y. L.; Boey, F.; Lam, Y. M. A new insight into controlling poly(3-hexylthiophene) nanofiber growth through a mixed-solvent approach for organic photovoltaics applications. *Journal of Materials Chemistry* **2011**, *21*, 377–386.

(4) Chen, D.; Nakahara, A.; Wei, D.; Nordlund, D.; Russell, T. P. P3HT/PCBM Bulk Heterojunction Organic Photovoltaics: Correlating Efficiency and Morphology. *Nano Letters* **2011**, *11*, 561–567.

(5) Fu, Y.; Lin, C.; Tsai, F.-Y. High field-effect mobility from poly(3-hexylthiophene) thin-film transistors by solventvapor-induced reflow. *Organic Electronics* **2009**, *10*, 883–888.

(6) Wang, J.; Zhang, F.; Zhang, M.; Wang, W.; An, Q.; Li, L.; Sun, Q.; Tang, W.; Zhang, J. Optimization of charge carrier transport balance for performance improvement of PDPP3T-based polymer solar cells prepared using a hot solution. *Physical Chemistry Chemical Physics* **2015**, *17*, 9835–9840.

(7) Masuda, K.; Ikeda, Y.; Ogawa, M.; Benten, H.; Ohkita, H.; Ito, S. Exciton Generation and Diffusion in Multilayered Organic Solar Cells Designed by Layer-by-Layer Assembly of Poly(p -phenylenevinylene). *ACS Applied Materials & Interfaces* **2010**, *2*, 236–245.

(8) Botiz, I.; Darling, S. B. Self-assembly of poly(3-hexylthiophene)-block-polylactide block

copolymer and subsequent incorporation of electron acceptor material. *Macromolecules* **2009**, *42*, 8211–8217.

(9) Lee, Y.-H.; Yen, W.-C.; Su, W.-F.; Dai, C.-A. Self-assembly and phase transformations of π-conjugated block copolymers that bend and twist: from rigid-rod nanowires to highly curvaceous gyroids. *Soft Matter* **2011**, *7*, 10429.

(10) Moon, H. C.; Bae, D.; Kim, J. K. Self-Assembly of Poly(3-dodecylthiophene)- block -poly(methyl methacrylate) Copolymers Driven by Competition between Microphase Separation and Crystallization. *Macromolecules* **2012**, *45*, 5201–5207.

(11) Lim, H.; Chao, C.-Y.; Su, W.-F. Modulating Crystallinity of Poly(3-hexylthiophene) via Microphase Separation of Poly(3-hexylthiophene)Polyisoprene Block Copolymers. *Macromolecules* **2015**, *48*, 3269–3281.

(12) Schmelz, J.; Schacher, F. H.; Schmalz, H. Cylindrical crystalline-core micelles: pushing the limits of solution self-assembly. *Soft Matter* **2013**, *9*, 2101.

(13) Hailes, R. L. N.; Oliver, A. M.; Gwyther, J.; Whittell, G. R.; Manners, I. Polyferrocenylsilanes: synthesis, properties, and applications. *Chemical Society Reviews* **2016**, *45*, 5358–5407.

(14) Cao, L.; Manners, I.; Winnik, M. A. Influence of the Interplay of Crystallization and Chain Stretching on Micellar Morphologies: Solution Self-Assembly of CoilCrystalline Poly(isoprene- block -ferrocenylsilane). *Macromolecules* **2002**, *35*, 8258–8260.

(15) Hsiao, M.-S.; Yusoff, S. F. M.; Winnik, M. A.; Manners, I. Crystallization-Driven Self-Assembly of Block Copolymers with a Short Crystallizable Core-Forming Segment: Controlling Micelle Morphology through the Influence of Molar Mass and Solvent Selectivity. *Macromolecules* **2014**, *47*, 2361–2372.

(16) Wang, X.; Guerin, G.; Wang, H.; Wang, Y.; Manners, I.; Winnik, M. A. Cylindrical block copolymer micelles and co-micelles of controlled length and architecture. *Science* **2007**, *317*, 644–7.

(17) Gilroy, J. B.; Rupar, P. A.; Whittell, G. R.; Chabanne, L.; Terrill, N. J.; Winnik, M. A.; Manners, I.; Richardson, R. M. Probing the structure of the crystalline core of field-aligned, monodisperse, cylindrical polyisoprene-block-polyferrocenylsilane micelles in solution using synchrotron small- and wide-angle X-ray scattering. *Journal of the American Chemical Society* **2011**, *133*, 17056–62.

(18) Finnegan, J. R.; Lunn, D. J.; Gould, O. E. C.; Hudson, Z. M.; Whittell, G. R.; Winnik, M. A.; Manners, I. Gradient Crystallization-Driven Self-Assembly: Cylindrical Micelles with Patchy Segmented Coronas via the Coassembly of Linear and Brush Block Copolymers. *Journal of the American Chemical Society* **2014**, *136*, 13835–13844.

(19) Qiu, H.; Gao, Y.; Du, V. A.; Harniman, R.; Winnik, M. A.; Manners, I. Branched micelles by living crystallization-driven block copolymer self-assembly under kinetic control. *Journal of the American Chemical Society* **2015**, *137*, 2375–85.

(20) Qiu, H.; Hudson, Z. M.; Winnik, M. A.; Manners, I. Multidimensional hierarchical self-assembly of amphiphilic cylindrical block comicelles. *Science* **2015**, *347*, 1329–1332.

(21) Li, X.; Gao, Y.; Boott, C. E.; Hayward, D. W.; Harniman, R.; Whittell, G. R.; Richardson, R. M.; Winnik, M. A.; Manners, I. Cross Supermicelles via the Hierarchical Assembly of Amphiphilic Cylindrical Triblock Comicelles. *Journal of the American Chemical Society* **2016**, *138*, 4087–4095.

(22) Yin, L.; Hillmyer, M. A. Disklike micelles in water from polyethylene-containing diblock copolymers. *Macromolecules* **2011**, *44*, 3021–3028.

(23) Schmelz, J.; Karg, M.; Hellweg, T.; Schmalz, H. General Pathway toward Crystalline-

Core Micelles with Tunable Morphology and Corona Segregation. *ACS Nano* **2011**, *5*, 9523–9534.

(24) Schmelz, J.; Schedl, A. E.; Steinlein, C.; Manners, I.; Schmalz, H. Length Control and Block-Type Architectures in Worm-like Micelles with Polyethylene Cores. *Journal of the American Chemical Society* **2012**, *134*, 14217–14225.

(25) Schöbel, J.; Karg, M.; Rosenbach, D.; Krauss, G.; Greiner, A.; Schmalz, H. Patchy Wormlike Micelles with Tailored Functionality by Crystallization-Driven Self-Assembly: A Versatile Platform for Mesostructured Hybrid Materials. *Macromolecules* **2016**, *49*, 2761–2771.

(26) Du, Z.-X.; Xu, J.-T.; Fan, Z.-Q. Micellar Morphologies of Poly(ϵ-caprolactone)- b -poly(ethylene oxide) Block Copolymers in Water with a Crystalline Core. *Macromolecules* **2007**, *40*, 7633–7637.

(27) Arno, M. C.; Inam, M.; Coe, Z.; Cambridge, G.; Macdougall, L. J.; Keogh, R.; Dove, A. P.; O'Reilly, R. K. Precision Epitaxy for Aqueous 1D and 2D Poly(ϵ-caprolactone) Assemblies. *Journal of the American Chemical Society* **2017**, *139*, 16980–16985.

(28) Park, S.-J.; Kang, S.-G.; Fryd, M.; Saven, J. G.; Park, S.-J. Highly tunable photoluminescent properties of amphiphilic conjugated block copolymers. *Journal of the American Chemical Society* **2010**, *132*, 9931–3.

(29) Patra, S. K.; Ahmed, R.; Whittell, G. R.; Lunn, D. J.; Dunphy, E. L.; Winnik, M. A.; Manners, I. Cylindrical micelles of controlled length with a π-conjugated polythiophene core via crystallization-driven self-assembly. *Journal of the American Chemical Society* **2011**, *133*, 8842–5.

(30) Gilroy, J. B.; Lunn, D. J.; Patra, S. K.; Whittell, G. R.; Winnik, M. A.; Manners, I. Fiber-like Micelles via the Crystallization-Driven Solution Self-Assembly

of Poly(3-hexylthiophene)- block -Poly(methyl methacrylate) Copolymers. *Macromolecules* **2012**, *45*, 5806–5815.

(31) Gwyther, J.; Gilroy, J. B.; Rupar, P. A.; Lunn, D. J.; Kynaston, E.; Patra, S. K.; Whittell, G. R.; Winnik, M. A.; Manners, I. Dimensional Control of Block Copolymer Nanofibers with a π-Conjugated Core: Crystallization-Driven Solution Self-Assembly of Amphiphilic Poly(3-hexylthiophene)- b -poly(2-vinylpyridine). *Chemistry - A European Journal* **2013**, *19*, 9186–9197.

(32) Qian, J.; Li, X.; Lunn, D. J.; Gwyther, J.; Hudson, Z. M.; Kynaston, E.; Rupar, P. A.; Winnik, M. A.; Manners, I. Uniform, High Aspect Ratio Fiber-like Micelles and Block Co-micelles with a Crystalline π-Conjugated Polythiophene Core by Self-Seeding. *Journal of the American Chemical Society* **2014**, *136*, 4121–4124.

(33) Kim, Y.-J.; Cho, C.-H.; Paek, K.; Jo, M.; Park, M.; Lee, N.-E.; Kim, Y.; Kim, B. J.; Lee, E. Precise Control of Quantum Dot Location within the P3HT- b -P2VP/QD Nanowires Formed by Crystallization-Driven 1D Growth of Hybrid Dimeric Seeds. *Journal of the American Chemical Society* **2014**, *136*, 2767–2774.

(34) He, L.; Pan, S.; Peng, J. Morphology control of poly(3-hexylthiophene)- b -poly(ethylene oxide) block copolymer by solvent blending. *Journal of Polymer Science Part B: Polymer Physics* **2016**, *54*, 544–551.

(35) Kynaston, E. L.; Gould, O. E. C.; Gwyther, J.; Whittell, G. R.; Winnik, M. A.; Manners, I. Fiber-Like Micelles from the Crystallization-Driven Self-Assembly of Poly(3-heptylselenophene)- block -Polystyrene. *Macromolecular Chemistry and Physics* **2015**, *216*, 685–695.

(36) Tao, D.; Feng, C.; Cui, Y.; Yang, X.; Manners, I.; Winnik, M. A.; Huang, X. Monodisperse Fiber-like Micelles of Controlled Length and Composition with an Oligo(p -

phenylenevinylene) Core via Living Crystallization-Driven Self-Assembly. *Journal of the American Chemical Society* **2017**, *139*, 7136–7139.

(37) Li, X.; Jin, B.; Gao, Y.; Hayward, D. W.; Winnik, M. A.; Luo, Y.; Manners, I. Monodisperse Cylindrical Micelles of Controlled Length with a Liquid-Crystalline Perfluorinated Core by 1D Self-Seeding. *Angewandte Chemie International Edition* **2016**, *55*, 11392–11396.

(38) Kamps, A. C.; Fryd, M.; Park, S.-J. Hierarchical self-assembly of amphiphilic semiconducting polymers into isolated, bundled, and branched nanofibers. *ACS Nano* **2012**, *6*, 2844–52.

(39) Ren, G.; Wu, P.-T.; Jenekhe, S. A. Solar Cells Based on Block Copolymer Semiconductor Nanowires: Effects of Nanowire Aspect Ratio. *ACS Nano* **2011**, *5*, 376–384.

(40) Iovu, M. C.; Craley, C. R.; Jeffries-EL, M.; Krankowski, A. B.; Zhang, R.; Kowalewski, T.; McCullough, R. D. Conducting Regioregular Polythiophene Block Copolymer Nanofibrils Synthesized by Reversible Addition Fragmentation Chain Transfer Polymerization (RAFT) and Nitroxide Mediated Polymerization (NMP). *Macromolecules* **2007**, *40*, 4733–4735.

(41) Choi, S. Y.; Lee, J. U.; Lee, J. W.; Lee, S.; Song, Y. J.; Jo, W. H.; Kim, S. H. Highly Ordered Poly(3-hexylthiophene) Rod Polymers via Block Copolymer Self-Assembly. *Macromolecules* **2011**, *44*, 1771–1774.

(42) Jin, S.-M.; Kim, I.; Lim, J. A.; Ahn, H.; Lee, E. Interfacial Crystallization-Driven Assembly of Conjugated Polymers/Quantum Dots into Coaxial Hybrid Nanowires: Elucidation of Conjugated Polymer Arrangements by Electron Tomography. *Advanced Functional Materials* **2016**, *26*, 3226–3235.

(43) Tu, G.; Li, H.; Forster, M.; Heiderhoff, R.; Balk, L. J.; Sigel, R.; Scherf, U. Am-

phiphilic conjugated block copolymers: Synthesis and solvent-selective photoluminescence quenching. *Small* **2007**, *3*, 1001–1006.

(44) Ho, C.-C.; Wu, S.-J.; Lin, S.-H.; Darling, S. B.; Su, W.-F. Kinetically Enhanced Approach for Rapid and Tunable Self-Assembly of Rod-Coil Block Copolymers. *Macromolecular Rapid Communications* **2015**, *36*, 1329–1335.

(45) Jeffries-El, M.; Sauvé, G.; McCullough, R. D. Facile Synthesis of End-Functionalized Regioregular Poly(3-alkylthiophene)s via Modified Grignard Metathesis Reaction. *Macromolecules* **2005**, *38*, 10346–10352.

(46) Iovu, M. C.; Jeffries-El, M.; Sheina, E. E.; Cooper, J. R.; McCullough, R. D. Regioregular poly(3-alkylthiophene) conducting block copolymers. *Polymer* **2005**, *46*, 8582–8586.

(47) Yokoyama, A.; Miyakoshi, R.; Yokozawa, T. Chain-Growth Polymerization for Poly(3-hexylthiophene) with a Defined Molecular Weight and a Low Polydispersity. *Macromolecules* **2004**, *37*, 1169–1171.

(48) Rodrigues, A.; Nabankur, D.; Hilliou, L.; Viana, J.; Bucknall, D. G.; Bernardo, G. Low temperature solid state processing of pure P3HT fibers. *AIP Advances* **2013**, *3*, 052116.

(49) Bernardo, G.; Nabankur, D.; Pereira, P.; Brandão, L.; Viana, J.; Bucknall, D. G. Solid-state low-temperature extrusion of P3HT ribbons. *Applied Physics A* **2014**, *117*, 2079–2086.

(50) Brinkmann, M.; Rannou, P. Effect of molecular weight on the structure and morphology of oriented thin films of regioregular poly(3-hexylthiophene) grown by directional epitaxial solidification. *Advanced Functional Materials* **2007**, *17*, 101–108.

(51) Wu, Z.; Petzold, A.; Henze, T.; Thurn-Albrecht, T.; Lohwasser, R. H.; Sommer, M.; Thelakkat, M. Temperature and Molecular Weight Dependent Hierarchical Equilibrium

Structures in Semiconducting Poly(3-hexylthiophene). *Macromolecules* **2010**, *43*, 4646–4653.

(52) Dudenko, D.; Kiersnowski, A.; Shu, J.; Pisula, W.; Sebastiani, D.; Spiess, H. W.; Hansen, M. R. A Strategy for Revealing the Packing in Semicrystalline π-Conjugated Polymers: Crystal Structure of Bulk Poly-3-hexyl-thiophene (P3HT). *Angewandte Chemie International Edition* **2012**, *51*, 11068–11072.

(53) Balko, J.; Lohwasser, R. H.; Sommer, M.; Thelakkat, M.; Thurn-Albrecht, T. Determination of the Crystallinity of Semicrystalline Poly(3-hexylthiophene) by Means of Wide-Angle X-ray Scattering. *Macromolecules* **2013**, *46*, 9642–9651.

(54) Colle, R.; Grosso, G.; Ronzani, A.; Zicovich-Wilson, C. M. Structure and X-ray spectrum of crystalline poly(3-hexylthiophene) from DFT-van der Waals calculations. *Physica Status Solidi B* **2011**, *248*, 1360–1368.

(55) Greasty, R. J.; Richardson, R. M.; Klein, S.; Cherns, D.; Thomas, M. R.; Pizzey, C.; Terrill, N.; Rochas, C. Electro-induced orientational ordering of anisotropic pigment nanoparticles. *Philosophical Transactions of the Royal Society A: Mathematical, Physical and Engineering Sciences* **2013**, *371*, 20120257.

(56) Causin, V.; Marega, C.; Marigo, A.; Valentini, L.; Kenny, J. M. Crystallization and Melting Behavior of Poly(3-butylthiophene), Poly(3-octylthiophene), and Poly(3-dodecylthiophene). *Macromolecules* **2005**, *38*, 409–415.

(57) Guérin, G.; Raez, J.; Manners, I.; Winnik, M. A. Light Scattering Study of Rigid, Rodlike Organometallic Block Copolymer Micelles in Dilute Solution. *Macromolecules* **2005**, *38*, 7819–7827.

(58) Gädt, T.; Ieong, N. S.; Cambridge, G.; Winnik, M. A.; Manners, I. Complex and hierarchical micelle architectures from diblock copolymers using living, crystallization-driven polymerizations. *Nature Materials* **2009**, *8*, 144–50.

(59) Machui, F.; Langner, S.; Zhu, X.; Abbott, S.; Brabec, C. J. Determination of the P3HT:PCBM solubility parameters via a binary solvent gradient method: Impact of solubility on the photovoltaic performance. *Solar Energy Materials and Solar Cells* **2012**, *100*, 138–146.

(60) Barton, A. F. M. Solubility parameters. *Chemical Reviews* **1975**, *75*, 731–753.

(61) Liu, J.; Arif, M.; Zou, J.; Khondaker, S. I.; Zhai, L. Controlling Poly(3-hexylthiophene) Crystal Dimension: Nanowhiskers and Nanoribbons. *Macromolecules* **2009**, *42*, 9390–9393.

(62) Gilroy, J. B.; Gädt, T.; Whittell, G. R.; Chabanne, L.; Mitchels, J. M.; Richardson, R. M.; Winnik, M. A.; Manners, I. Monodisperse cylindrical micelles by crystallization-driven living self-assembly. *Nature Chemistry* **2010**, *2*, 566–70.

(63) Melis, C.; Colombo, L.; Mattoni, A. Self-Assembling of Poly(3-hexylthiophene). *The Journal of Physical Chemistry C* **2011**, *115*, 576–581.

(64) Israelachvili, J. N. *Intermolecular and Surface Forces*; Elsevier, 2011; pp 503–534.

(65) Newbloom, G. M.; Kim, F. S.; Jenekhe, S. A.; Pozzo, D. C. Mesoscale Morphology and Charge Transport in Colloidal Networks of Poly(3-hexylthiophene). *Macromolecules* **2011**, *44*, 3801–3809.

(66) Hayward, D. W.; Gilroy, J. B.; Rupar, P. A.; Chabanne, L.; Pizzey, C.; Winnik, M. A.; Whittell, G. R.; Manners, I.; Richardson, R. M. Liquid Crystalline Phase Behavior of Well-Defined Cylindrical Block Copolymer Micelles Using Synchrotron Small-Angle X-ray Scattering. *Macromolecules* **2015**, *48*, 1579–1591.

(67) Hayward, D.; Whittell, G.; Gilroy, J.; Manners, I.; Richardson, R. An investigation into the hexagonal phases formed in high-concentration dispersions of well-defined cylindrical block copolymer micelles. *Liquid Crystals* **2016**, *43*, 1148–1159.

(68) Liu, J.; Sheina, E.; Kowalewski, T.; McCullough, R. D. Tuning the Electrical Conductivity and Self-Assembly of Regioregular Polythiophene by Block Copolymerization: Nanowire Morphologies in New Di- and Triblock Copolymers We gratefully acknowledge support from the NSF (CHE-9807707). *Angewandte Chemie International Edition* **2002**, *41*, 329.

(69) Iovu, M. C.; Jeffries-El, M.; Zhang, R.; Kowalewski, T.; McCullough, R. D. Conducting Block Copolymer Nanowires Containing Regioregular Poly(3-Hexylthiophene) and Polystyrene. *Journal of Macromolecular Science, Part A* **2006**, *43*, 1991–2000.

(70) Wu, Z.-Q.; Ono, R. J.; Chen, Z.; Bielawski, C. W. Synthesis of Poly(3-alkylthiophene)-block -poly(arylisocyanide): Two Sequential, Mechanistically Distinct Polymerizations Using a Single Catalyst. *Journal of the American Chemical Society* **2010**, *132*, 14000–14001.

(71) Higashihara, T.; Ueda, M. Living anionic polymerization of 4-vinyltriphenylamine for synthesis of novel block copolymers containing low-polydisperse poly(4-vinyltriphenylamine) and regioregular poly(3-hexylthiophene) segments. *Macromolecules* **2009**, *42*, 8794–8800.

(72) Sommer, M.; Lang, A. S.; Thelakkat, M. Crystalline-crystalline donor-acceptor block copolymers. *Angewandte Chemie International Edition* **2008**, *47*, 7901–7904.

(73) Schwarz, K. N.; Kee, T. W.; Huang, D. M. Coarse-grained simulations of the solution-phase self-assembly of poly(3-hexylthiophene) nanostructures. *Nanoscale* **2013**, *5*, 2017.

Graphical TOC Entry